ACS OMEGA

Open Access

http://pubs.acs.org/journal/acsodf

Article

Saponins Derived from the Korean Endemic Plant *Heloniopsis koreana* Inhibit Diffuse-type Gastric Cancer Cells

Su-Yeon Cho, Yejin Kim, Hoseong Hwang, Yujin Kwon, So-Ri Son, Jong Gwon Baek, InWha Park, Yoon Jin Kang, Hyungjin Rhee, Hak Cheol Kwon, Jaeyoung Kwon,* Won Kyu Kim,* and Dae Sik Jang*

Cite This: *ACS Omega* 2023, 8, 48019−48027

Read Online

ACCESS | Metrics & More | Article Recommendations | Supporting Information

ABSTRACT: Diffuse-type gastric cancer (GC) is a type of stomach cancer that occurs in small clusters of cells that are widely spread. It does not typically manifest with symptoms until the advanced stages and often goes undetected in routine imaging tests. In addition, there is no specific targeted therapy for diffuse-type GC and it has a high mortality risk. Hence, it is worthwhile to discover molecules against this cancer. In this study, the extract of *Heloniopsis koreana*, which is endemic to Korea, exhibited cytotoxicity against two diffuse-type GC cell lines, MKN1 and SNU668. This led to the isolation of 10 compounds, including a new cinnamic acid glycoside. Of the compounds, saponin Th (**4**) and SNF 11 (**5**) showed potent activities with IC_{50} values of 3.66 and 3.85 μM, respectively, in MKN1 cells, and 1.8 and 1.98 μM, respectively, in SNU668 cells. These compounds prevented cancer cell division, invasion, and colony formation in both cell lines. In addition, these compounds induced cancer cell death through conventional cell death pathways, showing an increase in ADP-ribose polymerase, caspase 3, and BAX and a decrease in BCL2.

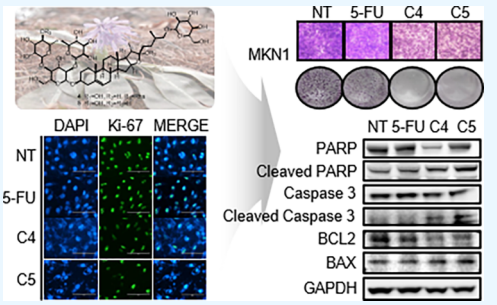

1. INTRODUCTION

Gastric cancer (GC) is the fifth most commonly diagnosed cancer and the fourth leading cause of cancer-related deaths worldwide.[1] According to the Lauren classification, GC is classified into two main histological subtypes: intestinal and diffuse types.[2] Intestinal-type GC is more prevalent in East Asian populations, whereas diffuse-type GC has a more uniform geographic occurrence.[3] While intestinal-type GC develops via atrophic gastritis and intestinal metaplasia and is mostly caused by *Helicobacter pylori* infection-mediated chronic inflammation,[4] the exact pathological mechanisms underlying the development of diffuse-type GC remain unclear. Recent studies by the Cancer Genome Atlas (TCGA) and the Asian Cancer Research Group (ACRG) have suggested that diffuse-type GC mostly belongs to a genomically stable subtype (TCGA) or an epithelial-to-mesenchymal transition (EMT) subtype, which usually shows frequent recurrence/metastasis and poor prognosis.[5,6] These studies also suggested some critical alterations in driver genes, such as CDH1, RHOA, and fusion genes between CLDN18-ARHGAP.[7−9] While CDH1 mutations are most frequently found in 30−50% of patients with diffuse-type GC, developing drugs against E-cadherin remains a challenge.[10] E-cadherin is a cell−cell adhesion protein encoded by CDH1; its critical roles in normal cells and complex regulatory mechanisms involving multiple factors make it a difficult target.[11] Diffuse-type GC is difficult to detect endoscopically because it grows without protruding or depressed lesions.[12] Patients with diffuse-type GC are frequently diagnosed with advanced-stage cancer, show HER2 expression less frequently than patients with intestinal-type GC, and consequently show poor responses to conventional chemotherapies based on fluoropyrimidine and platinum.[13] The most important pathological features of diffuse-type GC are frequent invasion and metastasis, which are directly associated with EMT character.[14] To date, most studies have tested the antiproliferative effects of various extracts and compounds in randomly organized GC cell line panels. However, it is important to establish an appropriate GC cell line panel based on EMT-related molecular marker expression and various assays reflecting the effects on not only cell growth but also the migratory activity of cancer cells to discover a compound particularly effective against diffuse-type GC.

Natural products are known to provide various health benefits such as high nutritional value, antioxidant properties, and anti-inflammatory and immune system enhancing effects. Plants synthesize an enormous variety of potent secondary metabolites consisting of numerous active or complementary compounds.[15] Natural products play an essential role in the

Received: September 5, 2023
Revised: November 10, 2023
Accepted: November 23, 2023
Published: December 6, 2023

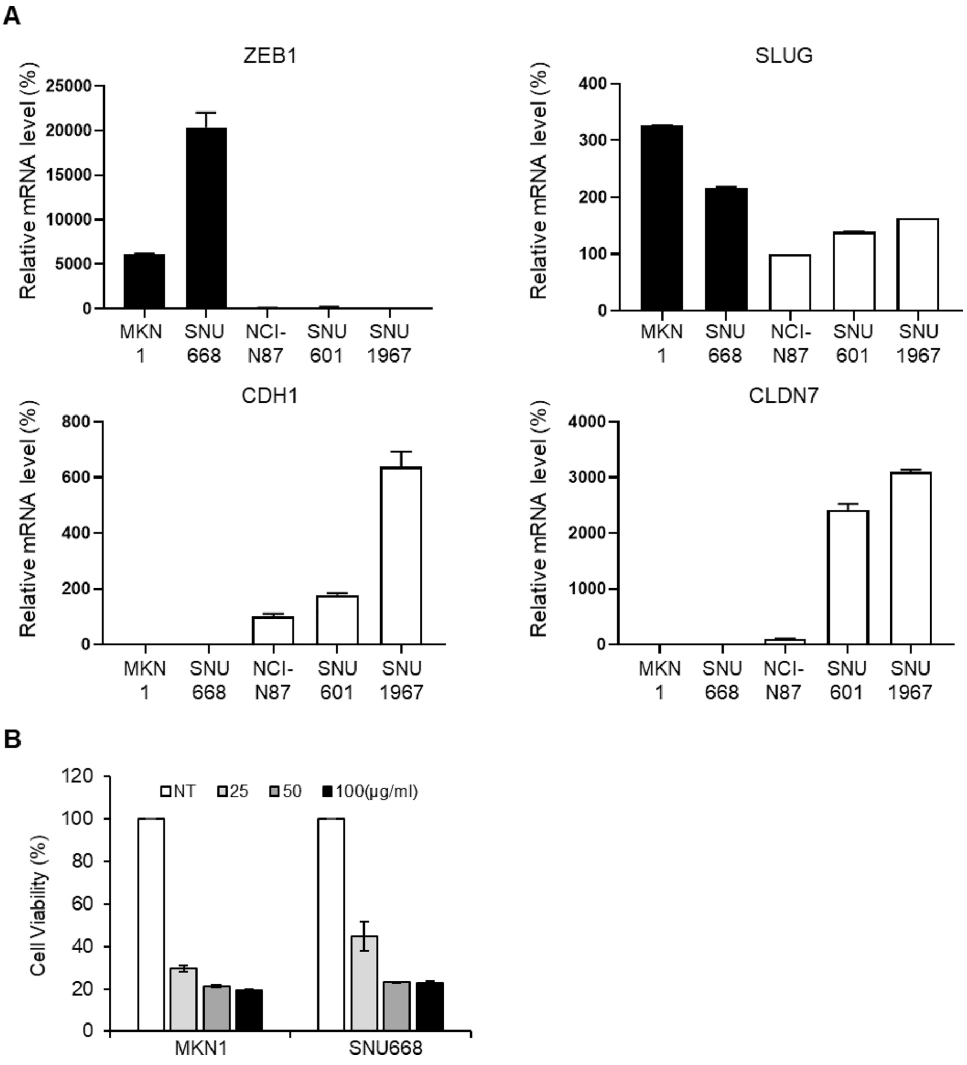

Figure 1. HKE inhibits cell growth in diffuse-type GC cells. (A) Expression of CDH1, Claudin-7, ZEB1, and SLUG was measured using qRT-PCR in MKN1, SNU668, NCI-N87, SNU601, and SNU1967 cells. (B) The MTT assay was performed on MKN1 and SNU668 cells treated with *Heloniopsis koreana* extract (HKE) (25, 50, and 100 μg/ml) for 72h.

treatment of human diseases. Furthermore, traditional remedies based primarily on indigenous plants still dominate treatment practices worldwide, and natural products constitute a large proportion of therapeutics today, especially in cancer treatment.[16] Many FDA-approved phytochemicals, such as taxol, etoposide, and camptothecin derivatives, have demonstrated significant anticancer potential.[17] Hence, the main purpose of this study was to discover various compounds from plant sources with potential activity against diffuse-type GC cell lines.

In the search for cytotoxic compounds against diffuse-type GC cell lines, preliminary screening for cytotoxicity was performed on locally endemic plants that are not well studied. Of the various plants, *Heloniopsis koreana* extract (HKE) showed the highest activity. *H. koreana*, also known as Cheonyeo-chi-ma, is an endemic herbaceous species found only in the north-central region of Korea.[18] The pink and purple flowers are grown for ornamental purposes. *H. koreana* is similar to *H. orientalis*, which is widely distributed in China and Japan but differs in its tepals and spatulate shape.[19] Although several studies have reported the isolation and analysis of steroidal saponins,[20] phenolic compounds,[21] and flavonoids[22] from *H. orientalis*, no studies have been conducted on the chemical components or biological activities of *H. koreana*. Herein, we report on the isolation, structural characterization, and biological evaluation of *H. koreana* compounds.

2. RESULTS AND DISCUSSION

2.1. Effect of *Heloniopsis koreana* Extract on Diffuse-Type Gastric Cancer Cells. We investigated the antitumorigenic effects of HKE on diffuse-type GC cells because diffuse-type GC poses a major challenge in clinical practice. To select diffuse-type GC cell lines, EMT markers (CDH1, CLDN7, ZEB1, and Slug) were analyzed in a panel of five GC cell lines. qPCR analysis showed that MKN1 and SNU668 cells exhibited inconsistent and strong EMT marker expression (Figure 1A). The effects of HKE on the cell growth of MKN1 and SNU668 cells were evaluated in a dose-dependent manner. The MTT assay showed that HKE treatment dramatically downregulated the growth of both GC cell lines, and this antiproliferative effect was saturated at a concentration of 50 μg/mL (Figure 1B).

2.2. Isolation and Structural Elucidation of the Compounds. As the activities of the fractions were not

https://doi.org/10.1021/acsomega.3c06714
ACS Omega 2023, 8, 48019−48027

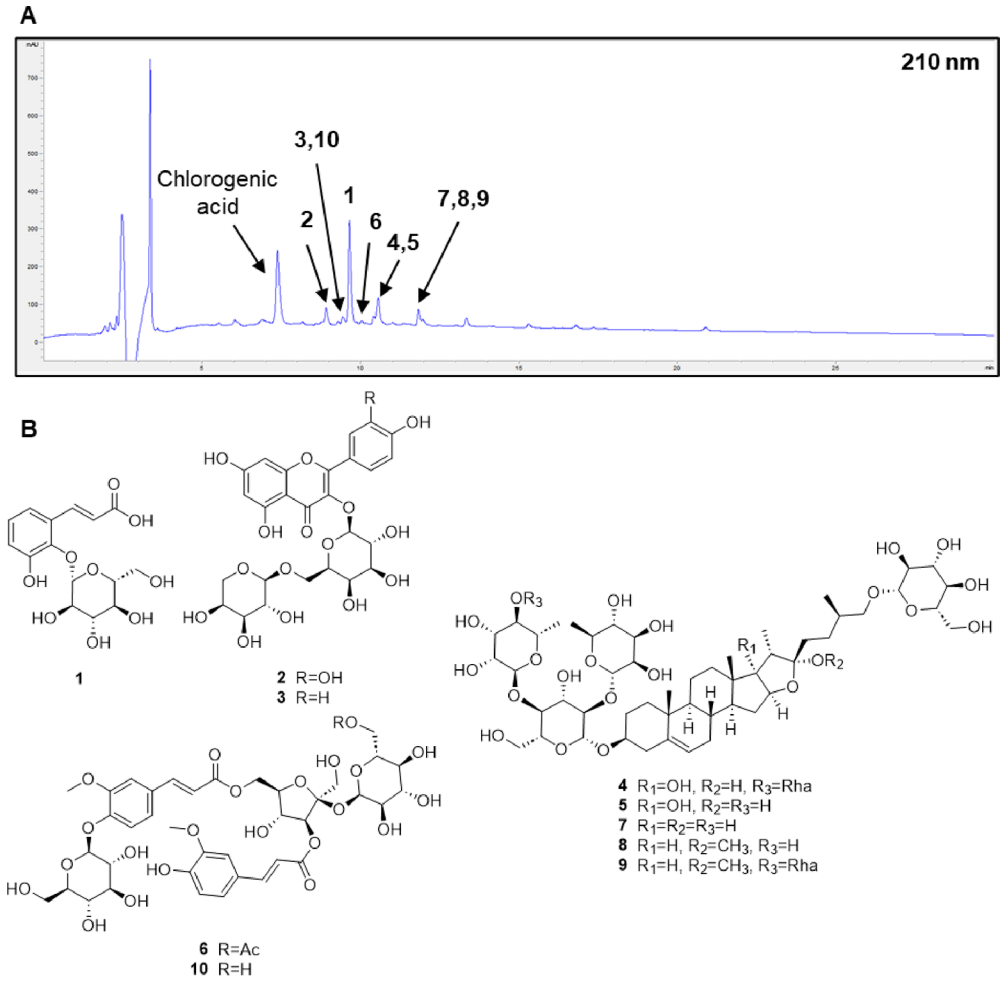

Figure 2. HPLC analysis of HKE and structures of compounds **1**–**10**. (A) HPLC chemical profiling of the *Heloniopsis koreana* extract (HKE) monitored by 210 nm. (B) The structures of 10 isolated compounds including a new cinnamic acid glycoside, two flavonoids, two phenylpropanoids, and five steroidal saponins.

significantly different, we analyzed the extract and fractions using liquid chromatography–mass spectrometry (LC-MS) (Figure 2A). The major compounds in the plant were distributed in both the *n*-butanol and water layers. The major compounds were steroidal saponins possessing furosta-5-ene-3,22,26-triol or its hydroxylated aglycones. The major compounds were isolated from the aqueous layer as it contained a large number of compounds. Ten compounds were isolated from the aqueous layer of HKE, and their structures were identified (Figure 2B).

Compound **1** was isolated as a white powder, and its molecular formula was established as $C_{15}H_{18}O_9$ by using high-resolution MS (HRMS) data. The infrared absorption spectrum revealed the presence of hydroxyl (3466 cm^{-1}), carboxyl (2913, 1721, 1291 cm^{-1}), olefinic (1635, 992 cm^{-1}), aromatic (1585, 1476 cm^{-1}), and ether (1031 cm^{-1}) groups. The ^1H NMR data (Table 1) showed three aromatic proton signals [6.93 (1H, dd, J = 8.0, 1.5 Hz, H-4), 7.04 (1H, t, J = 8.0 Hz, H-5), and 7.24 (1H, dd, J = 8.0, 1.5 Hz, H-6)], suggesting that they are part of an aromatic ring system and are likely adjacent to each other. These data also exhibited a *trans*-olefinic group [6.42 (1H, d, J = 16.0, H-8) and 8.24 (1H, d, J = 16.0, H-7)], implying that its aglycone could be a *trans*-2,3-dihydrocinnamic acid. The existence of the β-glucopyranosyl group was also indicated by analyzing the chemical shift and

Table 1. ^1H and ^{13}C NMR Data of Compound 1 in Dimethyl Sulfoxide-d_6

	1	
position	δ_C[a]	δ_H[b] [mult., (J in Hz)]
1	128.9	
2	144.0	
3	150.1	
4	118.5	6.93, dd (8.0, 1.5)
5	125.6	7.04, t (8.0)
6	117.1	7.24, dd (8.0, 1.5)
7	139.8	8.24, d (16.0)
8	119.5	6.42, d (16.0)
9	168.1	
1′	105.4	4.60, d (7.5)
2′	74.0	3.35, dd (9.0, 8.0)
3′	76.0	3.26, t (8.0)
4′	69.8	3.19, m
5′	77.3	3.19, m
6′	61.3	3.67, dd (12.0, 1.5)
		3.51, dd (12.0, 5.0)
3-OH		9.36, br s
9-OH		12.40, br s

[a]Recorded at 125 MHz. [b]Recorded at 500 MHz.

https://doi.org/10.1021/acsomega.3c06714
ACS Omega 2023, 8, 48019–48027

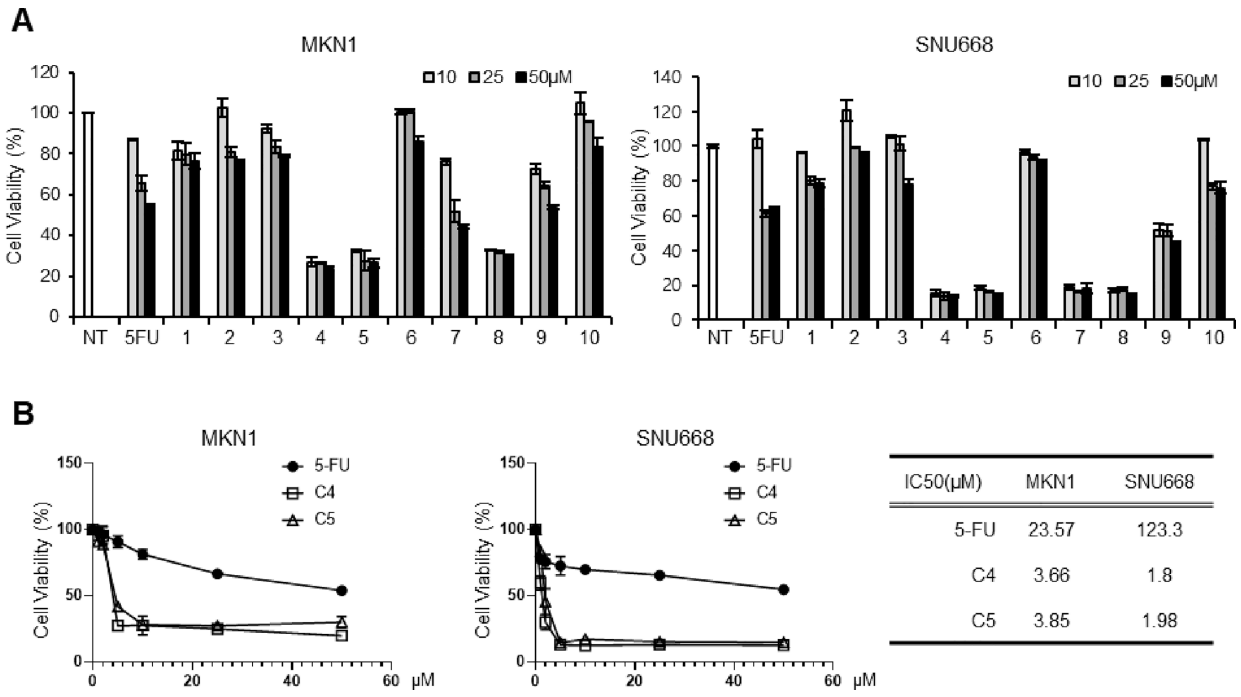

IC50(μM)	MKN1	SNU668
5-FU	23.57	123.3
C4	3.66	1.8
C5	3.85	1.98

Figure 3. Cell growth was measured in diffuse-type GC cell lines MKN1 and SNU668 using MTT analysis. (A) Ten *Heloniopsis koreana* extract (HKE)-derived compounds were tested at concentrations of 10, 25, and 50 μM for 72h. (B) C4 and C5 were tested at concentrations of 1, 2, 5, 10, 25, and 50 μM for 72h. 5-FU was used as a positive control. The IC_{50} value was calculated using the results from panel B.

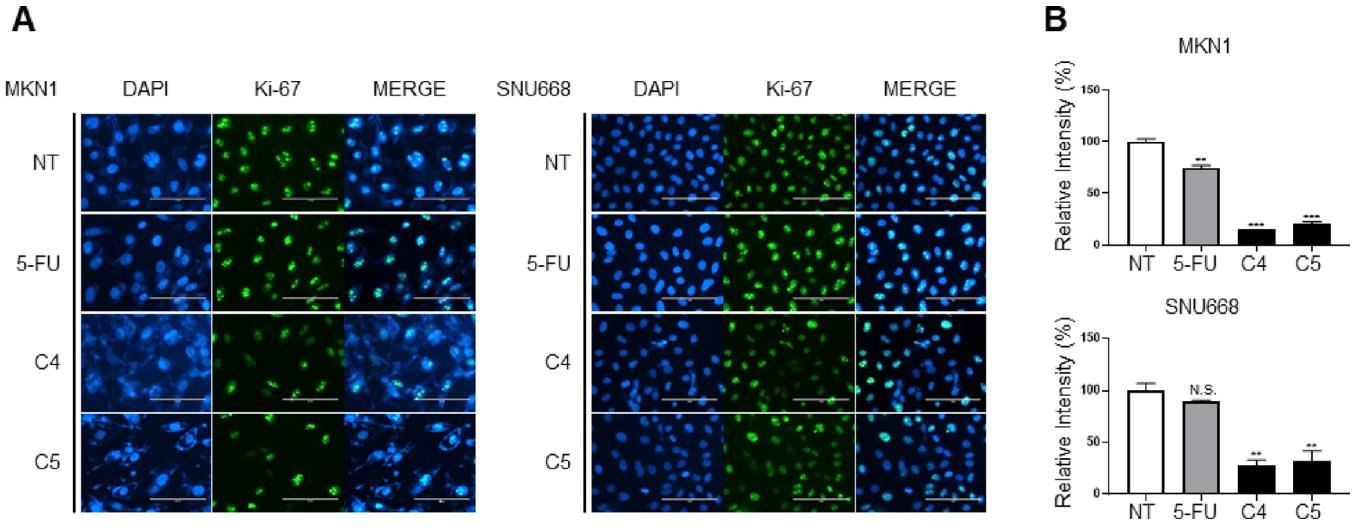

Figure 4. HKE-derived compounds suppress cancer cell proliferation by downregulating K_i-67 expression in diffuse-type GC cells. (A) Immunofluorescence microscopy analysis of K_i-67 was performed on MKN1 and SNU668 cells after treatment with 5 μM 5-FU, C4, and C5. (B) The relative fluorescence intensity of stained cells was quantified using ImageJ software. ***P <0.001, **P <0.01 vs the control.

coupling constant of an anomeric proton signal [4.60 (1H, d, J = 7.5 Hz, H-1′)] and signals at δ_H 3.19−3.67. The ^{13}C NMR data (Table 1) showed 15 carbon signals—two *trans*-olefinic carbon signals (δ_C 119.5, 139.8), three aromatic methine signals (δ_C 117.1, 118.5, 125.6), three quaternary carbons (δ_C 128.9, 144.0, 150.1) of an aromatic ring, one carboxyl carbon (δ_C 168.1), an anomeric carbon (δ_C 105.4), four methine carbons (δ_C 69.8, 74.0, 76.0, 77.3) of sugar, and one methylene carbon (δ_C 61.3). The COSY spectrum showed the correlations among H-4 (δ_H 6.93), H-5 (δ_H 7.04), and H-6 (δ_H 7.24) of the aromatic ring. The correlations between *trans*-olefinic proton signals and the proton signals of glucose were also observed. Through analysis of the HMBC spectrum, the position of glucose was determined as C-2 by observing the correlation of H-1′ (δ_H 4.60) with C-2 (δ_C 144.0). Furthermore, the glucose unit was determined to be in the D-form by acid hydrolysis using HPLC analysis (Figure S9). Thus, the structure of compound **1** was identified as 2-*O*-β-D-glucosyl-3-hydroxy-*trans*-cinnamic acid.

Compound **4** was isolated as a white amorphous powder. The UV data displayed weak absorption, attributable to the aglycone with little conjugation. LC-MS analysis revealed a molecular ion at m/z 1233.6 $[M + Na]^+$. Furthermore, the fragmentation patterns suggested that the steroidal aglycones contained five sugar units. The ^{1}H and ^{13}C NMR spectra showed characteristic signals for the aglycone and sugar units

https://doi.org/10.1021/acsomega.3c06714
ACS Omega 2023, 8, 48019−48027

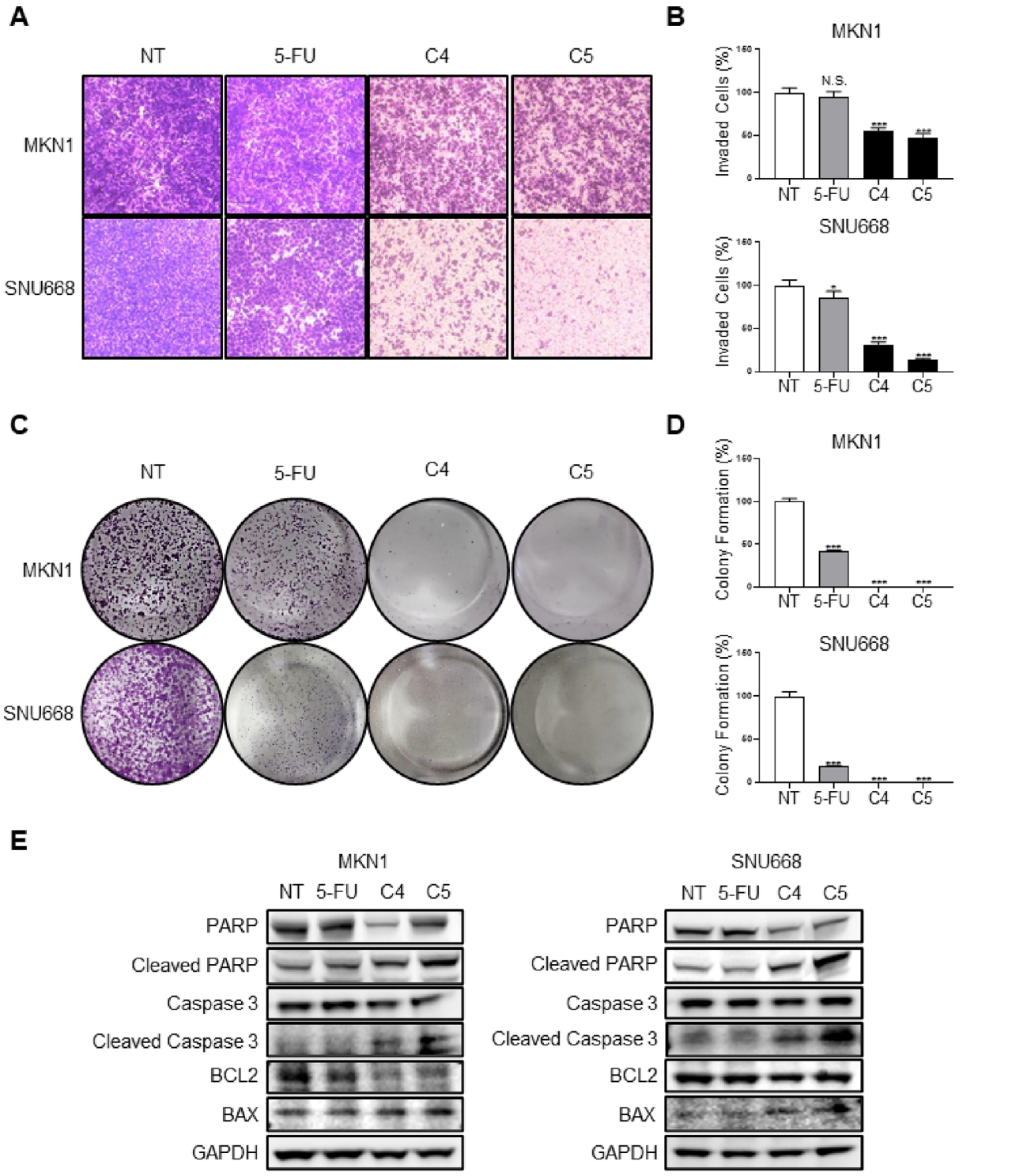

Figure 5. Antitumorigenic effects of HKE-derived compounds on invasion, stemness, and apoptosis in diffuse-type GC cells. (A) The invasion assay was performed on MKN1 and SNU668 cells after treatment with 5 μM 5-FU, C4, and C5 for 24 h. (C) The colony formation assay was performed on MKN1 and SNU668 cells after treatment with 5 μM 5-FU, C4, and C5 for 10 days. (B, D) Quantification of the relative number of stained cells using ImageJ software. (E) Western blot analysis was conducted to examine the levels of pro-apoptotic factors (PARP, cleaved-PARP, Caspase 3, Cleaved Caspase 3, and BAX) and an antiapoptotic factor (BCL2) in MKN1 and SNU668 cells treated with 10 μM 5-FU, C4, and C5 for 24 h. ***P <0.001, *P <0.05 vs the control.

because the spectra showed typical anomeric NMR signals for the sugar moieties (Figures S10 and S11). Compound **4** was identified as saponin Th because the remaining signals were consistent with those previously reported for saponin Th.[23] Compound **5** was isolated as a white amorphous powder, and its structure was determined similar to that of compound **4**. LC-MS analysis revealed a molecular ion at m/z 1087.5 $[M + Na]^+$, and the fragmentation patterns implied that this compound consisted of the same aglycone and five sugar units. After a detailed analysis of the NMR spectra and

https://doi.org/10.1021/acsomega.3c06714
ACS Omega 2023, 8, 48019−48027

comparison with the literature (Figures S12 and S13), compound **5** was identified as SNF 11.[24]

The other known compounds were identified as rumarin (**2**),[25] 3-[(6-O-α-L-arabinopyranosyl-β-D-galactopyranosyl)-oxy]-5,7-dihydroxy-2-(4-hydroxyphenyl)-4*H*-1-benzopyran-4-one (**3**),[26] helonioside D (**6**),[21] protodioscin (**7**),[27] methyl-protodioscin (**8**),[28] methyldichotomin (**9**),[29] and helonioside C (**10**),[21] by comparison with their NMR spectrum and previously published data. Various saponins and phenolic compounds have previously been isolated from the genus *Heloniopsis*. To the best of our knowledge, this study marks the first isolation of compounds **2**−**5**, **7**, and **8** from the genus *Heloniopsis*.

2.3. Effect of Isolated Compounds on Diffuse-Type Gastric Cancer Cells. The effects of all isolated compounds were tested at different doses by using the MTT assay, and 5-FU was used as a positive control. Of the 10 compounds, compounds **4** and **5** showed the strongest antiproliferative effects on both GC cell lines, whereas compounds **7**−**9** showed variable effects. The antiproliferative effects of compounds **4** and **5** were saturated at a concentration of 10 μM (Figure 3A). The IC_{50} values of these compounds were further analyzed. The IC_{50} values of 5-FU, compound **4**, and compound **5** were 23.57, 3.66, and 3.85 μM, respectively, in MKN1 cells, and 123.3, 1.8, and 1.98 μM, respectively, in SNU668 cells (Figure 3B). K_i-67, one of the best-known prognostic markers of GC, was further analyzed to evaluate the effects of compounds **4** and **5** on cell division. Immunofluorescence microscopy showed a strong decrease in K_i-67 intensity in GC cells treated with compounds **4** and **5** (5 μM) (Figure 4A,B).

2.4. Abrogation of Aggressive Diffuse-Type GC Cell Phenotypes and Activation of Conventional Apoptosis. Most cancer-related deaths are attributed to the metastasis of primary tumors to proximal and distal organs, and frequent metastasis is a particularly challenging problem in diffuse-type GC.[14] Hence, the effects of compounds **4** and **5** on the invasive activity of MKN1 and SNU668 cells were assessed. Both compounds showed strong inhibitory effects on the invasion of GC cells (Figures 5A and 4B). The effects of these compounds were further evaluated on colony formation in GC cells because the colony formation ability is related to drug resistance and stemness. Treatment with compounds **4** and **5** completely prevented colony formation in both the GC cell lines (Figure 5C,D). In addition, from a mechanistic perspective, we investigated whether compound-induced cancer cell death was mediated by conventional cell death pathways. Western blot analysis showed that the expression of pro-apoptotic factors such as activated forms of PARP, caspase 3, and BAX was evidently increased by treatment with compounds **4** and **5** whereas that of the antiapoptotic factor BCL2 was decreased in both diffuse GC cell lines (Figure 5E). These results indicate that compounds **4** and **5** induced cell death in diffuse-type GC cells through the conventional apoptotic pathway.

3. CONCLUSIONS

The goal of this study was to identify HKE-derived compounds effective against selected diffuse-type GC cells based on EMT marker expression. Among the isolated compounds, compounds **4** and **5** showed the strongest inhibitory activity against diffuse-type GC cells, demonstrating significantly stronger antitumor effects than 5-FU, a standard therapeutic regimen for patients with diffuse-type GC. Even at low concentrations ranging from 1.8 to 3.85 μM, compounds **4** and **5** induced 50% cell death in both MKN1 and SNU668 cells. In contrast, the IC_{50} values of 5-FU were relatively high, at 23.57 μM for MKN1 and 123.3 μM for SNU668. The downregulation of Ki67 expression and upregulation of apoptosis marker expression induced by treatment with compounds **4** and **5** suggest that cell death mediated by these compounds was at least partially caused by the induction of nuclear damage, cell cycle arrest, and activation of the conventional caspase-mediated apoptosis pathway. Owing to the strong antiproliferative activity of these compounds, the invasion assay was performed only at 24 h post-treatment. Both diffuse-type GC cell lines exhibited strong migratory activity after 24 h, indicating that these cell lines exhibited EMT-like features. The treatment with compounds **4** and **5** drastically perturbed the migratory ability in both cell lines, while 5-FU showed a little inhibitory effect. In addition to displaying EMT-like features, diffuse-type GC cells exhibit a challenging phenotype characterized by stem cell-like behaviors, including poor response to chemotherapeutic regimens.[30,31] Treatment with compounds **4** and **5** almost completely inhibited colony formation in both MKN1 and SNU668 cells, indicating that these compounds robustly reduce the stem cell population of diffuse-type GC cells. In future studies, it will be important to investigate the specific targets of these compounds and their simultaneous inhibition of cell growth, invasive activity, and stemness. Considering their strong cytotoxicity, a combination of these compounds with targeted delivery technologies, such as exosomes and antibody-conjugated drugs, can be considered for *in vivo* applications.

4. MATERIALS AND METHODS

4.1. General Experimental Procedures. Diaion HP-20 resin (Mitsubishi Chemical Industries, Ltd., Tokyo, Japan), Sephadex LH-20 gel (GE Healthcare, Stockholm, Sweden), silica gel (230−400 mesh; Merck, Kenilworth, MA, USA), and LiChroprep RP-18 gel (40−63 mm; Merck) were used for open-column chromatography. The fractions were monitored by thin-layer chromatography on silica gel 60 F254 (Merck) and RP-18 F254S (Merck) plates. MPLC (Teledyne Isco, Lincoln, NE, USA) was used for further fractionation using prepacked Redi Sep-Silica (Teledyne Isco). Preparative HPLC was performed using an HPLC purification system (1525 pump and PDA 1996 detector, Waters Corp., Milford, MA, USA) with a Gemini NX-C18 110A (250 × 21.2 mm inner diameter, 5 μm, Phenomenex, Torrance, CA, USA). UV and Fourier transform infrared (FT-IR) spectra were recorded using OPTIZEN UV−vis and Agilent Cary 630 FT-IR (Agilent Technologies, Santa Clara, CA, USA) spectrophotometers, respectively. Optical rotations were measured using a JASCO P-2000 polarimeter; nuclear magnetic resonance (NMR) spectra were acquired by JEOL (JEOL, Tokyo, Japan) at 500 MHz, and high-resolution mass spectrometry (HRMS) data were obtained via a Q-exactive high-resolution mass spectrometer (Thermo Fisher Scientific Inc., Waltham, MA, USA).

4.2. Plant Material and Extraction. *Heloniopsis koreana* Fuse, N.S. Lee, and M.N. Tamura were collected from Mt. Taegi (Hoengseong-gun, Gangwon-do, Republic of Korea) in September 2021 and identified by Jung Hwa Kang of the Hantaek Botanical Garden. A voucher specimen (SJ00005A) has been deposited at the KIST Gangneung Institute of Natural Products. Whole plants of *Heloniopsis koreana* Fuse,

https://doi.org/10.1021/acsomega.3c06714
ACS Omega 2023, 8, 48019−48027

N.S. Lee, and M.N. Tamura (1.4 kg) were dried and chopped (214.5 g). The dried plant was extracted with 70% EtOH/water (2 × 2.2 L) for 7 days at room temperature and evaporated under reduced pressure to obtain an *H. koreana* crude extract (HKE, 57.2 g).

4.3. Isolation of Compounds. HKE was suspended in water and successively partitioned with *n*-hexane (3 × 300 mL) and *n*-BuOH (2 × 300 mL) to yield *n*-hexane-soluble (2.7 g), *n*-BuOH-soluble (15.3 g), and water-soluble (37.3 g) layers. The water-soluble layer (37.30 g) was fractionated over column chromatography using Diaion HP-20 (ϕ 5.4 × 34.0 cm) as a stationary phase with a gradient system of methanol (MeOH)/H_2O (0/100 to 100/0, v/v) to give eight fractions (F1−F8). F3 was divided further by Sephadex LH-20 (ϕ 2.6 × 68.8 cm, MeOH/H_2O = 4/6) and produced 14 fractions (F3-1−F3-14). Compound **10** (9.5 mg) was isolated from F3-8 by carrying out preparative HPLC [Column: GEMINI C18 (20.0 × 250 mm), solvent: H_2O (A), MeOH (B), 35% B (100 min) → 50% B (80 min), flow rate: 7.0 mL/min]. F3-9 was separated by silica MPLC (40 g, CH_2Cl_2/MeOH/H_2O = 90/9/1 → 50/45/5, v/v/v) to obtain compound **1** (142.8 mg). F3-12 was subjected to silica MPLC (12 g, CH_2Cl_2/MeOH/H_2O = 90/9/1 → 60/36/4, v/v/v) to yield compounds **2** (21.2 mg) and **3** (4.0 mg). F4 was fractionated using Sephadex LH-20 (ϕ 2.6 × 63.4 cm, MeOH/H_2O = 5/5) and produced eight fractions (F4-1 ∼ F4-8). F4-3 was subjected to silica MPLC (12 g, CH_2Cl_2/MeOH/H_2O = 90/9/1 → 60/36/4, v/v/v), and compound **6** (4.0 mg) was obtained. F5 was separated by silica gel CC (ϕ 3.7 × 32.0 cm, EtOAc/MeOH/H_2O = 70/25/5, v/v/v) and produced five fractions (F5-1−F5-5). F5-1 was divided by Lichoprep C18 CC (ϕ 3.7 × 34.3 cm, MeOH/H_2O = 55/45) and gained eight fractions (F5-1-1−5-1-8). F5-1-4 was subjected to silica gel CC (ϕ 3.8 × 25.0 cm, $CHCl_3$/MeOH/H_2O = 7/4/1) to get compounds **4** (328.0 mg) and **5** (29.0 mg). F6 was further fractionated using silica gel CC (ϕ 2.5 × 40.6 cm, CH_2Cl_2/MeOH/H_2O = 80/18/2, v/v/v) and yielded three fractions (F6-1−F6-3). Compound **7** (344.8 mg) was obtained from F6-2 by repeated chromatography including silica gel CC (ϕ 3.8 × 25.0 cm, $CHCl_3$/MeOH/H_2O = 7/4/1). Conducting silica gel CC of F6-3 (ϕ 2.7 × 27.0 cm, $CHCl_3$/MeOH/H_2O = 80/35/5) led to the isolation of compounds **8** (30.7 mg) and **9** (45.4 mg).

4.3.1. 2-O-β-D-Glucosyl-3-hydroxy-trans-cinnamic Acid (1). White powder; $[\alpha]^{22}_D$ +105.8 (*c* 0.1, MeOH); UV (MeOH) λ_{max} nm (log ε) 232 (4.04), 285 (4.06); IR (ATR) ν_{max} 3466, 2913, 1721, 1635, 1585, 1476, 1291, 1191, 1031, 992, 786, 743 cm^{-1}; ^1H and ^{13}C NMR data (see Table 1); HRESIMS (positive mode) *m*/*z* 365.0834 $[M+Na]^+$ (calcd for $C_{15}H_{18}O_9Na$, 365.0843).

4.3.2. Saponin Th (4). White amorphous powder; ^1H and ^{13}C NMR spectra (pyridine-d_5) (see Figures S10 and S11); ESI-MS (positive) *m*/*z* 1233.6 $[M + Na]^+$.

4.3.3. SNF 11 (5). White amorphous powder; ^1H and ^{13}C NMR spectra (pyridine-d_5) (see Figures S12 and S13); and ESI-MS (positive) *m*/*z* 1087.5 $[M + Na]^+$.

4.4. Cell Culture and Reagents. The MKN1 and SNU668 cell lines were purchased from the Korean Cell Line Bank (Cancer Research Institute, Seoul, Republic of Korea) and maintained in the Roswell Park Memorial Institute (RPMI) medium containing 10% fetal bovine serum (FBS) and 1% penicillin/streptomycin (P/S) at 37 °C in a 5% CO_2 incubator. GC cells treated with 5-fluorouracil (5-FU) (Tocris, Ellisville, MO, USA) were used as a positive control.

4.5. Cell Viability Assay. Cell viability was analyzed using the 3-(4,5-dimethylthiazol-2-yl)-2,5-diphenyl-2*H*-tetrazolium bromide (MTT) assay. MKN1 and SNU668 cells were seeded in 96-well plates at a density of 1 × 10^4 cells/well and treated with 5-FU, HKE, and the isolated compounds at different doses. MTT (5 mg/mL) was added to the plates, and the mixture was incubated at 37 °C for 4 h. The formazan crystals were dissolved with DMSO, and the OD was measured at 570 nm by using a microplate reader. IC_{50} values were calculated using the online tool Quest Graph IC_{50} Calculator (AAT Bioquest, Inc., Sunnyvale, CA, USA; https://www.aatbio.com/tools/ic50-calculator).

4.6. Western Blotting. Whole-cell lysates were prepared by using passive lysis buffer (Promega, Madison, WI, USA) with a protease inhibitor cocktail (Roche, Basel, Switzerland). The proteins were electrophoresized and transferred onto a membrane. The membranes were incubated overnight at 4 °C with primary antibodies against Poly (ADP-ribose) polymerase (PARP), cleaved-PARP, caspase 3, cleaved caspase 3, BCL2 (Cell Signaling Technology, Beverly, MA, USA), BAX (Santa Cruz Biotechnology), and GAPDH (Trevigen, Gaithersburg, MD, USA). The membranes were washed and incubated with the appropriate secondary antibodies for 1 h at room temperature. Western blot images were analyzed by using a LAS 4000 mini camera (Fujifilm, Tokyo, Japan).

4.7. Immunofluorescence. Cells grown on slides were rinsed with phosphate-buffered saline (PBS), fixed with 4% paraformaldehyde for 30 min, and permeabilized with 0.2% Triton X-100 in PBS. The slides were incubated overnight at 4 °C with primary antibody against K_i-67 (Abcam, Cambridge, UK). The slides were then incubated for 1 h with the appropriate fluorescence-labeled secondary antibodies (Life Technologies, Carlsbad, CA, USA). All images were collected using an Operetta High-Content Imaging System (PerkinElmer, Waltham, MA, USA).

4.8. Invasion Assay. The QCM 24-well cell invasion assay kit (Millipore, Burlington, MA, USA) was used according to the manufacturer's guidelines. Briefly, the inset interiors were rehydrated with prewarmed serum-free media, and 0.2 × 10^6 cells were added to each insert. The complete medium (10% FBS) with 5 μM 5-FU, compound **4**, or compound **5** was added to the lower chambers, and the cells were incubated for 24 h in a CO_2 incubator. The cells were then stained with a 0.5% crystal violet solution, and images were obtained using the 10× objective of an Olympus BX51 microscope (Olympus, Tokyo, Japan) and an IX71 camera.

4.9. Colony Formation Assay. MKN1 and SNU668 cells were seeded in 24-well plates (5000 cells/well). The plates were cultured for 10 days with 5 μM 5-FU, compound **4**, or compound **5** in a 5% CO_2 incubator at 37 °C. The medium was changed every 3 days. Cells were then washed with PBS and stained with a 0.5% crystal violet solution for 20 min. The number of cell colonies was manually quantified by using ImageJ software (NIH).

4.10. Quantitative Reverse Transcription PCR (RT-qPCR). Total RNA was extracted using the Illustra RNAspin Mini kit (GE Healthcare, Chicago, IL, USA) according to the manufacturer's instructions. Reverse transcription was performed with 2 μg of total RNA using the M-MLV reverse transcriptase (Life Technologies, Carlsbad, CA, USA). Subsequently, RT-qPCR was performed using SYBR Premix Ex *Taq*II (TaKaRa Biotechnology, Dalian, China) and the QuantStudio 6 Pro System (Applied Biosystems, Carlsbad,

https://doi.org/10.1021/acsomega.3c06714
ACS Omega 2023, 8, 48019−48027

CA, USA). All reactions were performed in triplicates. The following oligonucleotide primer sets were used: CDH1 forward: 5′-CGAGAGCTACACGTTCACGG-3′, reverse: 5′-GGGTGTCGAGGGAAAAATAGG-3′; Claudin-7 forward: 5′-AGCTGCAAAATGTACGACTCG-3′, reverse: 5′-GGAGACCACCATTAGGGCTC-3′; ZEB1 forward, 5′-TTACACCTTTGCATACAGAACCC-3′, reverse: 5′-TTTACGATTACACCCAGACTGC-3′; Slug forward: 5′-CGAACTGGACACACATACAGTG-3′, reverse: 5′-CTGAGGATCTCTGGTTGTGGT-3′; GAPDH forward: 5′-GGAGCGAGATCCCTCCAAAAT-3′, reverse: 5′-GGCTGTTGTCATACTTCTCATGG-3′.

4.11. Statistical Analysis. Data are presented as means ± SD, and all experiments were performed at least three times. For statistical analysis, one-way analysis of variance (ANOVA) and Student's *t* test were performed using GraphPad Prism 7.0 (La Jolla, CA, USA), and significant differences were confirmed by Tukey's multiple comparison test. Statistical significance was set at $P < 0.05$.

■ ASSOCIATED CONTENT

Supporting Information

The Supporting Information is available free of charge at https://pubs.acs.org/doi/10.1021/acsomega.3c06714.

HRESIMS, IR, UV, ^{1}H, ^{13}C, and 2D NMR data of compound **1**; sugar determination; and ^{1}H and ^{13}C NMR data of compounds **4** and **5**(PDF)

■ AUTHOR INFORMATION

Corresponding Authors

Jaeyoung Kwon − *KIST Gangneung Institute of Natural Products, Korea Institute of Science and Technology, Gangneung 25451, Republic of Korea; Division of Bio-Medical Science &Technology, KIST School, University of Science and Technology, Seoul 02792, Republic of Korea;* orcid.org/0000-0002-8706-2305; Email: kjy1207@kist.re.kr

Won Kyu Kim − *KIST Gangneung Institute of Natural Products, Korea Institute of Science and Technology, Gangneung 25451, Republic of Korea; Department of Medical Science, Yonsei University Wonju College of Medicine, Wonju 26426, Republic of Korea*; Email: wkkim@kist.re.kr

Dae Sik Jang − *Department of Biomedical and Pharmaceutical Sciences, Graduate School and College of Pharmacy, Kyung Hee University, Seoul 02447, Republic of Korea;* orcid.org/0000-0001-5472-5232; Email: dsjang@khu.ac.kr

Authors

Su-Yeon Cho − *KIST Gangneung Institute of Natural Products, Korea Institute of Science and Technology, Gangneung 25451, Republic of Korea; Division of Bio-Medical Science &Technology, KIST School, University of Science and Technology, Seoul 02792, Republic of Korea*

Yejin Kim − *Department of Biomedical and Pharmaceutical Sciences, Graduate School and College of Pharmacy, Kyung Hee University, Seoul 02447, Republic of Korea*

Hoseong Hwang − *KIST Gangneung Institute of Natural Products, Korea Institute of Science and Technology, Gangneung 25451, Republic of Korea*

Yujin Kwon − *KIST Gangneung Institute of Natural Products, Korea Institute of Science and Technology, Gangneung 25451, Republic of Korea; Division of Bio-Medical Science &Technology, KIST School, University of Science and Technology, Seoul 02792, Republic of Korea*

So-Ri Son − *Department of Biomedical and Pharmaceutical Sciences, Graduate School and College of Pharmacy, Kyung Hee University, Seoul 02447, Republic of Korea*

Jong Gwon Baek − *KIST Gangneung Institute of Natural Products, Korea Institute of Science and Technology, Gangneung 25451, Republic of Korea*

InWha Park − *KIST Gangneung Institute of Natural Products, Korea Institute of Science and Technology, Gangneung 25451, Republic of Korea*

Yoon Jin Kang − *KIST Gangneung Institute of Natural Products, Korea Institute of Science and Technology, Gangneung 25451, Republic of Korea*

Hyungjin Rhee − *Department of Radiology, Research Institute of Radiological Science, Center for Clinical Imaging Data Science, Severance Hospital, Yonsei University College of Medicine, Seoul 03722, Republic of Korea*

Hak Cheol Kwon − *KIST Gangneung Institute of Natural Products, Korea Institute of Science and Technology, Gangneung 25451, Republic of Korea;* orcid.org/0000-0002-4071-2331

Complete contact information is available at: https://pubs.acs.org/10.1021/acsomega.3c06714

Author Contributions

VS.-Y.C., Y.K., and H.H. contributed equally to this work. The manuscript was written through the contributions of all authors. All authors have approved the final version of the manuscript.

Notes

The authors declare no competing financial interest.

■ ACKNOWLEDGMENTS

This research was funded by the Korea Institute of Science and Technology Program (grant numbers 2E32641 and 2E32641-23-079) and the National Research Foundation of Korea (grant number 2020R1C1C1003887).

■ REFERENCES

(1) Sung, H.; Ferlay, J.; Siegel, R. L.; Laversanne, M.; Soerjomataram, I.; Jemal, A.; Bray, F. Global cancer statistics 2020: GLOBOCAN estimates of incidence and mortality worldwide for 36 cancers in 185 countries. *CA Cancer J. Clin.* **2021**, *71* (3), 209−249.

(2) Monster, J. L.; Kemp, L. J.; Gloerich, M.; van der Post, R. S. Diffuse gastric cancer: Emerging mechanisms of tumor initiation and progression. *Biochim. Biophys. Acta, Rev. Cancer* **2022**, *1877*, No. 188719.

(3) Rahman, R.; Asombang, A. W.; Ibdah, J. A. Characteristics of gastric cancer in Asia. *World J. Gastroenterol.* **2014**, *20* (16), 4483.

(4) Uemura, N.; Okamoto, S.; Yamamoto, S.; Matsumura, N.; Yamaguchi, S.; Yamakido, M.; Taniyama, K.; Sasaki, N.; Schlemper, R. J. Helicobacter pylori infection and the development of gastric cancer. *N. Engl. J. Med.* **2001**, *345* (11), 784−789.

(5) Tan, P.; Yeoh, K.-G. Genetics and molecular pathogenesis of gastric adenocarcinoma. *Gastroenterology* **2015**, *149* (5), 1153−1162.e3.

(6) Cristescu, R.; Lee, J.; Nebozhyn, M.; Kim, K.-M.; Ting, J. C.; Wong, S. S.; Liu, J.; Yue, Y. G.; Wang, J.; Yu, K.; Ye, X. S.; Do, I.-G.; Liu, S.; Gong, L.; Fu, J.; Jin, J. G.; Choi, M. G.; Sohn, T. S.; Lee, J. H.; Bae, J. M.; Kim, S. T.; Park, S. H.; Sohn, I.; Jung, S.-H.; Tan, P.; Chen,

R.; Hardwick, J.; Kang, W. K.; Ayers, M.; Hongyue, D.; Reinhard, C.; Loboda, A.; Kim, S.; Aggarwal, A. Molecular analysis of gastric cancer identifies subtypes associated with distinct clinical outcomes. *Nat. Med.* **2015**, *21* (5), 449−456.
(7) van der Post, R. S.; Vogelaar, I. P.; Carneiro, F.; Guilford, P.; Huntsman, D.; Hoogerbrugge, N.; Caldas, C.; Chelcun Schreiber, K. E.; Hardwick, R. H.; Ausems, M. G. E. M.; Bardram, L.; Benusiglio, P. R.; Bisseling, T. M.; Blair, V.; Bleiker, E.; Boussioutas, A.; Cats, A.; Coit, D.; DeGregorio, L.; Figueiredo, J.; Ford, J. M.; Heijkoop, E.; Hermens, R.; Humar, B.; Kaurah, P.; Keller, G.; Lai, J.; Ligtenberg, M. J. L.; O'Donovan, M.; Oliveira, C.; Pinheiro, H.; Ragunath, K.; Rasenberg, E.; Richardson, S.; Roviello, F.; Schackert, H.; Seruca, R.; Taylor, A.; ter Huurne, A.; Tischkowitz, M.; Joe, S. T. A.; van Dijck, B.; van Grieken, N. C. T.; van Hillegersberg, R.; van Sandick, J. W.; Vehof, R.; van Krieken, J. H.; Fitzgerald, R. C. Hereditary diffuse gastric cancer: updated clinical guidelines with an emphasis on germline *CDH1* mutation carriers. *J. Med. Genet.* **2015**, *52* (6), 361−374.
(8) Zhang, H.; Schaefer, A.; Wang, Y.; Hodge, R. G.; Blake, D. R.; Diehl, J. N.; Papageorge, A. G.; Stachler, M. D.; Liao, J.; Zhou, J.; Wu, Z.; Akarca, F. G.; de Klerk, L. K.; Derks, S.; Pierobon, M.; Hoadley, K. A.; Wang, T. C.; Church, G.; Wong, K. K.; Petricoin, E. F.; Cox, A. D.; Lowy, D. R.; Der, C. J.; Bass, A. J. Gain-of-function *RHOA* mutations promote focal adhesion kinase activation and dependency in diffuse gastric cancer. *Cancer Discovery* **2020**, *10* (2), 288−305.
(9) Zhang, W.-H.; Zhang, S.-Y.; Hou, Q.-Q.; Qin, Y.; Chen, X.-Z.; Zhou, Z.-G.; Shu, Y.; Xu, H.; Hu, J.-K. The significance of the *CLDN18-ARHGAP* fusion gene in gastric cancer: a systematic review and meta-analysis. *Front. Oncol.* **2020**, *10*, 1214.
(10) Luo, W.; Fedda, F.; Lynch, P.; Tan, D. CDH1 gene and hereditary diffuse gastric cancer syndrome: molecular and histological alterations and implications for diagnosis and treatment. *Front. Pharmacol.* **2018**, *9*, 1421.
(11) Guo, X.; Zhao, F.; Ma, X.; Shen, G.; Ren, D.; Zheng, F.; Du, F.; Wang, Z.; Ahmad, R.; Yuan, X.; Zhao, J.; Zhao, J. A comparison between triplet and doublet chemotherapy in improving the survival of patients with advanced gastric cancer: a systematic review and meta-analysis. *BMC Cancer* **2019**, *19* (1), 1−14.
(12) Lee, J. Y.; Gong, E. J.; Chung, E. J.; Park, H. W.; Bae, S. E.; Kim, E. H.; Kim, J.; Do, Y. S.; Kim, T. H.; Chang, H.-S.; Song, H. J.; Choe, J.; Jung, H.-Y. The characteristics and prognosis of diffuse-type early gastric cancer diagnosed during health check-ups. *Gut Liver* **2017**, *11* (6), 807.
(13) Ooki, A.; Yamaguchi, K. The dawn of precision medicine in diffuse-type gastric cancer. *Ther. Adv. Med. Oncol.* **2022**, *14*, 175883592210830.
(14) Huang, L.; Wu, R.-L.; Xu, A.-M. Epithelial-mesenchymal transition in gastric cancer. *Am. J. Transl. Res.* **2015**, *7* (11), 2141.
(15) Najmi, A.; Javed, S. A.; Al Bratty, M.; Alhazmi, H. A. Modern approaches in the discovery and development of plant-based natural products and their analogues as potential therapeutic agents. *Molecules* **2022**, *27* (2), 349.
(16) Newman, D. J.; Cragg, G. M. Natural products as sources of new drugs over the nearly four decades from 01/1981 to 09/2019. *J. Nat. Prod.* **2020**, *83* (3), 770−803.
(17) Singh, S.; Sharma, B.; Kanwar, S. S.; Kumar, A. Lead phytochemicals for anticancer drug development. *Front. Plant Sci.* **2016**, *7*, 1667.
(18) Tanaka, N. Taxonomy, evolution and phylogeography of the genus *Helonias* (Melanthiaceae) revisited. *Phytotaxa* **2019**, *390* (1), 1−84.
(19) Fuse, S.; Sook Lee, N. N.; Tamura, M. N. Biosystematic studies on the genus Heloniopsis (Melanthiaceae) II. Two new species from Korea based on morphological and molecular evidence. *Taxon* **2004**, *53* (4), 949−958.
(20) Nakano, K.; Murakami, K.; Takaishi, Y.; Tomimatsu, T.; Nohara, T. Studies on the constituents of *Heloniopsis orientalis* (Thunb.) C. Tanaka. *Chem. Pharm. Bull.* **1989**, *37* (1), 116−118.
(21) Nakano, K.; Murakami, K.; Takaishi, Y.; Tomimatsu, T. Feruloyl sucrose derivatives from *Heloniopsis orientalis*. *Chem. Pharm. Bull.* **1986**, *34* (12), 5005−5010.
(22) Park, H.-J.; Min, B.-M.; Cha, H.-C. Flavonoid analysis of *Heloniopsis orientalis* (Thunb.) by high performance liquid chromatography. *J. Plant Biol.* **2003**, *46*, 250−254.
(23) Wang, B.; Zhang, J.; Pang, X.; Yuan, J.; Yang, J.; Yang, Y.; Gao, L.; Zhang, J.; Fan, Z.; He, L.; Yue, W.; Li, Y.; Pei, X.; Ma, B. Furostanol saponins from *trillium tschonoskii* promote the expansion of human cord blood hematopoietic stem and progenitor cells. *J. Nat. Prod.* **2020**, *83* (9), 2567−2577.
(24) Ando, J.; Miyazono, A.; Zhu, X.-H.; Ikeda, T.; Nohara, T. Studies on the constituents of solanaceous plants, steroidal glycosides from *Solanum nodiflorum*. *Chem. Pharm. Bull.* **1999**, *47* (12), 1794−1796.
(25) Takemura, M.; Nishida, R.; Mori, N.; Kuwahara, Y. Acylated flavonol glycosides as probing stimulants of a bean aphid, *Megoura crassicauda*, from *Vicia angustifolia*. *Phytochemistry* **2002**, *61* (2), 135−140.
(26) Yoshitama, K.; Ishikura, N.; Maso, T.; Oka, S.; Kai, M.; Uchino, A. The flavonoid chemistry of the genus *Trillium*: I. Flavonol glycosides in the leaves of *Trillium tschonoskii* maxim. and their geographical variations. *Bot. mag. Tokyo* **1992**, *105*, 555−563.
(27) Hu, K.; Dong, A.; Yao, X.; Kobayashi, H.; Iwasaki, S. Antineoplastic agents II: four furostanol glycosides from rhizomes of *Dioscorea collettii* var. *hypoglauca*. *Planta Med.* **1997**, *63* (02), 161−165.
(28) Cheng, M. S.; Wang, Q. L.; Tian, Q.; Song, H. Y.; Liu, Y. X.; Li, Q.; Xu, X.; Miao, H. D.; Yao, X. S.; Yang, Z. Total synthesis of methyl protodioscin: a potent agent with antitumor activity. *J. Org. Chem.* **2003**, *68* (9), 3658−3662.
(29) Yang, D.-J.; Lu, T.-J.; Hwang, L. S. Isolation and identification of steroidal saponins in Taiwanese yam cultivar (*Dioscorea pseudojaponica* Yamamoto). *J. Agric. Food Chem.* **2003**, *51* (22), 6438−6444.
(30) Guo, R.; Chu, A.; Gong, Y. Identification of cancer stem cell-related biomarkers in intestinal-type and diffuse-type gastric cancer by stemness index and weighted correlation network analysis. *J. Transl. Med.* **2020**, *18* (1), 1−14.
(31) Li, Y.; Wang, Z.; Ajani, J. A.; Song, S. Drug resistance and Cancer stem cells. *Cell Commun. Signaling* **2021**, *19* (1), 1−11.

https://doi.org/10.1021/acsomega.3c06714
ACS Omega 2023, 8, 48019−48027